



ANALYSIS OF SPATIAL AND TEMPORAL CHANGES IN LAND COVER AND LAND USE: THE CASE STUDY OF KOCAELI-KANDIRA

Erhan YILDIRIM^{1*} Özer AKYÜREK¹

¹ Department of Geomatics, Engineering Faculty, Kocaeli University, Türkiye.

* Corresponding Author: E. Yıldırım, ✉ erhanteias@gmail.com  0009-0002-8055-2229

ABSTRACT

The ability to accurately determine land cover change and the direction of change provides the scientific basis for policy implementation and predictable urban planning, and is one of the most reliable sources of data. The utilisation of cloud-based platforms, such as Google Earth Engine (GEE), facilitates the acquisition of all satellite data monitoring our planet, thereby offering substantial advantages. This facilitates specific or global analyses of each region, enabling such studies to be conducted with minimal effort. This study examines the district of Kandıra in Kocaeli province, which has undergone significant land use transformation in recent years due to increasing pressure from transport, urbanisation, industrialisation for food production and tourism. The amount and spatial character of the transformation in question were analyzed between 2017 and 2024. In this regard, the Random Forest classifier executed on Sentinel-2 satellite images on the Google Earth Engine platform was cross-validated with the Landsat-based LandTrendr time series algorithm. The analysis revealed that 2,503 hectares of agricultural land in the study area had been converted to artificial land. When comparing the results of two different algorithms, the spatial overlap between the methods was calculated as 0.1041 using the Jaccard Similarity Index; the parcel-based details of the classification method and the complementary role of LandTrendr in capturing vegetation damage were revealed. When examining the spatial characteristics of the change, it was determined that new developments were concentrated at an average distance of 727 meters from the Rural Housing Areas designated in the 1/25,000 scale Master Development Plan. This finding proves that the transformation in Kandıra is not a random scattering (leap-frog/outlying), but rather follows a spread model defined in the literature as Edge Expansion, which extends beyond the boundaries of planned rural settlements, and that the pressure of unplanned construction is concentrated on agricultural lands.

Keywords: Land Use/Land Cover Change, LandTrendr, Google Earth Engine, Edge-Expansion, Plan Incompatibility.

Cited As:

Yıldırım, E. & Akyürek, Ö. (2026). Analysis of Spatial and Temporal Changes in Land Cover and Land Use: The Case Study of Kocaeli-Kandıra, *Advances in Geomatics*, 4(1), 83-105.
<https://doi.org/10.5281/zenodo.20558376>

1. INTRODUCTION

A significant challenge confronting Türkiye in the 21st century pertains to the interplay between demographic mobility and spatial planning, a dynamic that has contributed to the proliferation of unsustainable urbanisation practices. The process defined as the ruralization of cities rather than the urbanization of villagers in the sociological perspective manifests itself in the spatial dimension as infrastructure deficiencies, lack of disaster resilience, and crises in resource management (Kongar, 2002). Especially in metropolitan areas such as Kocaeli, where industry and agriculture are intertwined, this phenomenon manifests itself in the form of distorted urbanization and urban sprawl, with the pressure of unplanned expansion irreversibly intensifying on productive agricultural land. Since traditional mapping methods are insufficient for monitoring the scale of this rapid transformation and the damage to agricultural land, Remote Sensing (RS) technologies and Geographic Information Systems (GIS) have become indispensable tools for accurately detecting large-scale changes in land cover and land use. Indeed, the literature emphasizes that changes in land cover trigger environmental risks associated with rapid urbanization and deforestation (Drummond & Loveland, 2010; Agaton et al., 2016), leading to ecological degradation such as loss of biodiversity (Butt et al., 2015).

Nowadays, satellite imagery, and especially multispectral images that capture data across various electromagnetic spectrum bands, have made it possible to map land cover in great detail on a large scale (Tirmanoglu et al., 2023; Rogan & Chen, 2004). Satellite imagery reveals surface characteristics that are crucial for numerous studies, including agricultural monitoring, urban planning, and environmental research (Li et al., 2020; Gu et al., 2021). On the other hand, understanding not only the extent of land change but also its formation process (trend) is vital for sustainable planning. Time series algorithms based on the Landsat remote sensing system have been developed to determine whether the pressure on agricultural and forest areas is a sudden break or a gradual deterioration over time. Among these algorithms, Landsat-based Detection of Trends in Disturbance and Recovery (LandTrendr) can model vegetation loss and recovery processes with high accuracy through its annual pixel-based analysis capability (Kennedy et al., 2010).

Traditional remote sensing methods are generally based on comparing images from two different dates and may be insufficient in fully reflecting the historical process and dynamics of change. To overcome this limitation and process large volumes of satellite data more quickly, the cloud-based computing platform Google Earth Engine (GEE) has become a revolutionary tool for researchers in recent years (Gorelick et al., 2017). GEE allows for high-accuracy land cover classification and change detection across large areas thanks to the integration of machine learning algorithms (such as Random Forest) (Ghorbanian et al., 2020).

The literature contains a large number of studies that look at changes in land cover. Griffiths et al. (2013), used the LandTrendr algorithm with high accuracy to determine the transition of all land

cover changes, as well as the change in agricultural land across Europe, in addition to the issue of abandoned deforestation. Huang et al. (2017), used the entire Landsat archive on the GEE platform to map land cover dynamics in a complex metropolitan area such as Beijing, demonstrating the high success and speed of cloud-based algorithms in tracking urban sprawl. Kennedy et al. (2018), used GEE modules developed for the implementation of the LandTrendr algorithm in a cloud-based architecture and for fast execution on large datasets. Nguyen (2020), analyzed land cover change in Vietnam's northwestern region between 2003 and 2010 using Landsat imagery on the GEE platform. In his study, he used the Classification and Regression Tree (CART) classification method to determine land cover classes and provided useful information about land cover change in Dien Bien province and the mechanisms of this change. Chen et al. (2021), examined land use changes in China's Bohai Rim coastal region using long-term time series analyses on the GEE platform. Their analyses highlighted that the greatest loss occurred in agricultural areas. They found that the land cover lost from agricultural areas was mostly converted into residential areas, cities, and port structures. Pande (2022), analyzed land use/cover changes in India's Rahuri watershed area using GEE. Using Landsat and Sentinel satellite imagery, he analyzed land use/land cover values for the years 2010, 2015, and 2020 on the GEE platform using the Random Forest classification method. As a result of his analyses, he determined the amount of change for each land cover/land use class. Teja et al. (2024), studied changes in land cover/use in India's Telangana state between 2002 and 2015 using Landsat-7 and Sentinel-2 imagery via the GEE cloud platform. Okoduwa and Amaechi (2024), used the GIS and GEE platform to analyze land cover changes in Nigeria's Abuja region. Using Landsat-8 remote sensing images, they classified land classes with 92% overall accuracy using a Random Forest classification algorithm, identifying land cover/use changes between 2014 and 2023.

This study aims to examine the loss of forest and agricultural land in the Kandıra district of Kocaeli province using a multidimensional approach. The study primarily aims to analyze remote sensing images and the LandTrendr algorithm to determine the temporal change in forest and agricultural areas within the Kandıra district. Afterwards, based on the principle that the spatial distribution of land change is not random, but rather that nearby objects are more related, as stated in Tobler's First Law of Geography, the spatial dependency of change on distance from existing settlement centers was analyzed. In this context, whether urban growth exhibits the characteristic of Edge Expansion has been tested using the approaches proposed by Li and Yeh (2004). In order to systematically characterize this spatial dependency, the urban growth typology proposed by Li and Yeh (2004) provides a foundational framework. Li and Yeh (2004) proposed a conceptual framework for understanding urban expansion, distinguishing between three distinct spatial patterns: infilling, edge-expansion, and leapfrog development. These patterns were based on the topological relationship between newly developed patches and existing urban boundaries. The integration of this conceptual approach is of crucial importance to the present study, since it formally determines whether the loss of agricultural land in Kandıra is driven by contiguous outward growth from existing villages (edge-expansion) or

by fragmented, disconnected sprawl (leapfrog). The study aims to reveal the spatial and temporal dynamics of rural-urban transformation in the case of Kandira by using Sentinel-2 and Landsat data with a hybrid methodology.

2. MATERIALS AND METHODS

The materials and methods used in the study are described in this section. The workflow methodology created for the implementation of all these methods is shown in Figure 1.

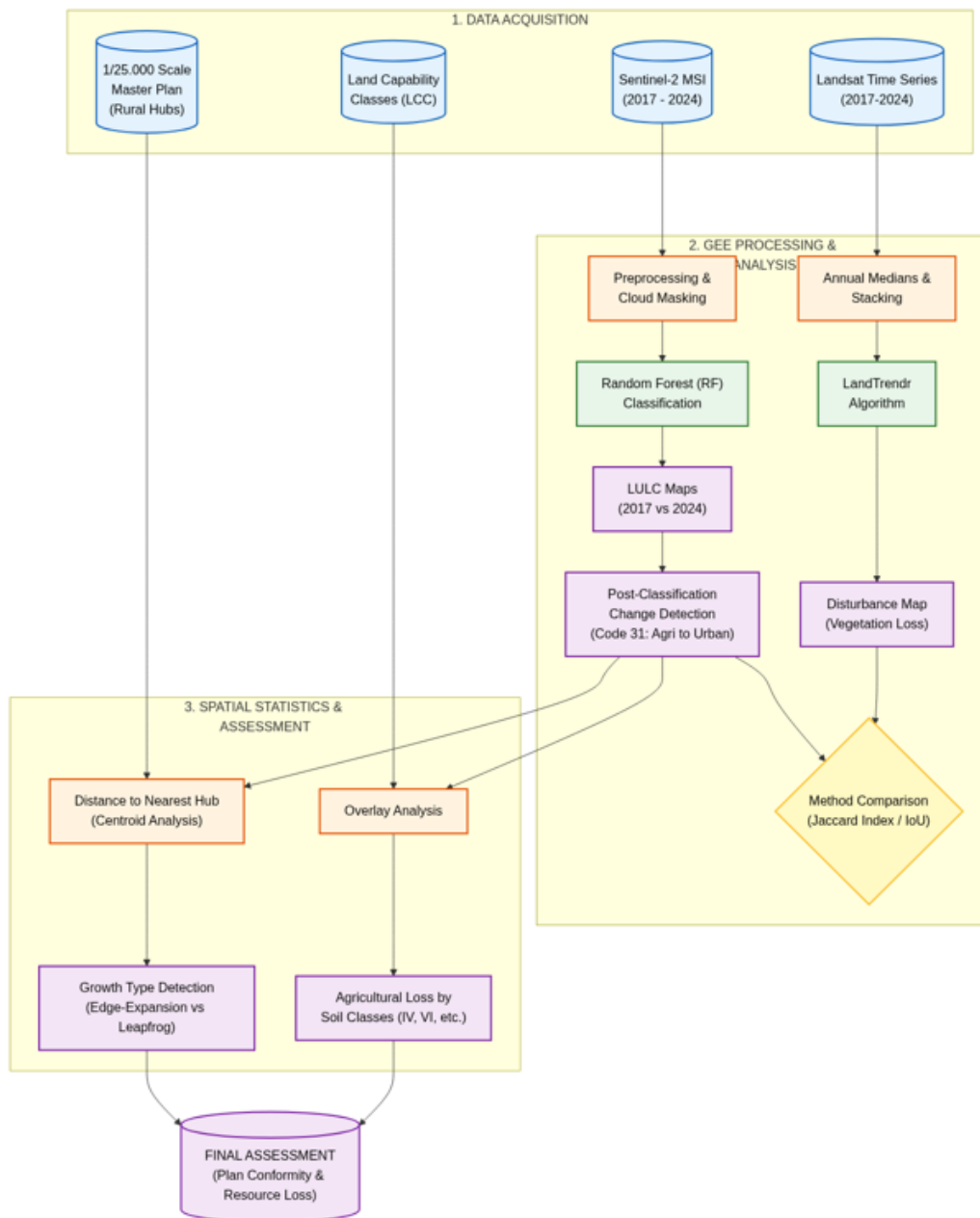


Figure 1. Workflow methodology for the study.

2.1 Study Area

Kandıra, the district with the largest agricultural area in Kocaeli Province, was selected as the study area for this study (Figure 2). Kandıra is located in the northeast of Kocaeli and is the largest district in the province with an area of 933 km². The district, located on the Black Sea coast, stands out for its fertile agricultural lands and natural beauty. The district's geographical coordinates range between 41° 04' N and 30° 09' E. The elevation of the district center above sea level is 75 meters. The district's climate is impacted by the climate of the Western Black Sea and Marmara regions. While it does not have a stable climate, it exhibits transitional climate characteristics. Rainfall in summer is generally irregular. Winters are generally not very cold, with rainfall mostly in the form of rain and little snowfall. Forests stretching along the coastline cover a significant area of the district (Kandıra District Governor's Office, 2025).

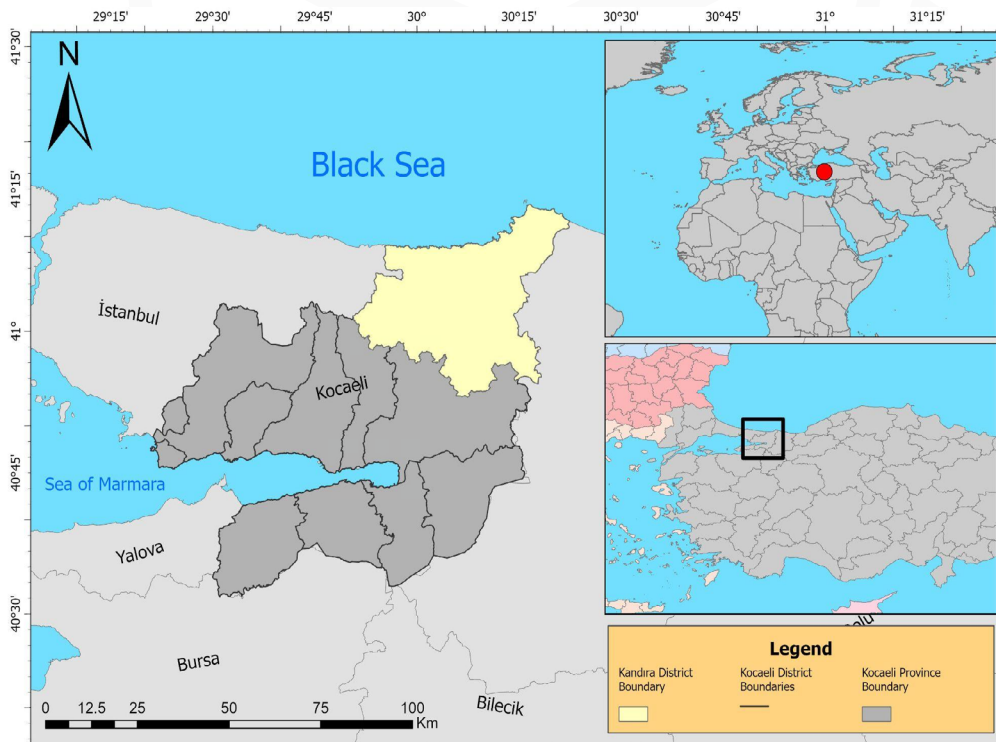


Figure 2. Study area.

2.2 Datasets

In this study, remote sensing data and spatial planning data were integrated to monitor land use dynamics in the Kandıra district and analyze trends in unplanned construction. European Space Agency (ESA) Sentinel-2 MSI satellite multispectral image bands ('B2', 'B3', 'B4', 'B8', 'B11', 'B12' and three widely used spectral indices were calculated and added to the model as independent variables: NDVI, NDWI, NDBI; spatial texture metrics were not included) were used to monitor changes in the study area during the 2017–2024 period. These data, with a spatial resolution of 10 meters, were processed

on the GEE platform and formed the basis for Random Forest classification. Images were filtered for the summer season and cloud masking was applied using the QA60 band. Landsat 8 satellite images were used to verify land change trends from a long-term perspective. These data were evaluated using the LandTrendr algorithm to model the historical process of vegetation loss. To determine the agricultural nature of areas undergoing transformation, Land Capability Classes (LCC) maps were obtained from the Ministry of Agriculture and Forestry database. This dataset has been used to determine whether areas removed from agriculture are absolute agricultural land. The 1/25,000 scale Master Development Plan data, approved by the Kocaeli Metropolitan Municipality, was also used to define the legal and planned settlements in the working area. The boundaries designated as Rural Residential Areas under the plan have been accepted as Reference Centers (Hubs) in spatial analyses. Any development identified outside these boundaries has been assessed as potential Degradation/Unplanned Development.

2.3 Methods

A multi-stage methodology was followed to identify changes in land cover/use in the study area and to analyze the spatial dynamics driving these changes. The first stage involved GEE-based image processing and time series analysis, followed by change detection and validation, spatial statistical analyses, and finally land suitability/proximity analyses. The processing of large-scale Sentinel-2 and Landsat satellite image collections, the creation of annual image composites, and the execution of the LandTrendr algorithm were carried out using the cloud-based Google Earth Engine (GEE) platform and ArcGIS Pro software, respectively. To ensure a rigorous accuracy assessment, reference validation samples were collected completely independent of the training dataset, preventing any potential data leakage. Ground truth reference data for both training and validation areas were derived from high-resolution orthophotos for the year 2017, and from high-resolution Google Earth imagery for the year 2024. This multi-source verification confirms the high reliability of the classification results. The final adjustments to the change maps, spatial statistical calculations, and map designs were performed using QGIS v3.40 desktop software. All spatial data and analysis outputs have been standardized in the WGS84 / UTM Zone 35N (EPSG: 32635) coordinate system for areal and positional accuracy, in accordance with the geographical location of Kocaeli province.

A Distance to Nearest Hub analysis was applied to determine the spatial pattern of land conversion. In this context, the Euclidean distance between each pixel converted from agriculture to artificial land between 2017 and 2024 and the centroid of the nearest village or neighborhood settlement area was calculated. The frequency distribution (histogram) and measures of central tendency (mean and median) of the obtained distance values were used to determine whether the growth type was Leapfrog or Edge-Expansion.

The Jaccard Similarity Index (Intersection over Union - IoU) was used to determine the spatial overlap

level between the results of the Sentinel-2-based classification (Random Forest) and the Landsat-based time series (LandTrendr) analyses applied in the study. In computer vision and image processing literature, IoU is preferred as a standard metric for measuring object detection and segmentation performance, particularly because it does not include unchanged background areas (True Negatives) in the success criterion (Szeliski, 2022).

$$IoU = \frac{\text{Area of Intersection}}{\text{Area of Union}} \quad (1)$$

In this regard, the index calculated by dividing the intersection area of the change maps produced by two different algorithms using Equation (1) by the union area was used to reveal the extent to which the methods validate or complement each other.

2.3.1. Remote Sensing and Time Series Analysis

The analysis process was initiated by processing Sentinel-2 satellite images on the GEE cloud platform. Cloud masking and atmospheric correction processes were applied to the image collection covering the 7-year period between 2017 and 2024, and median composite images best representing the study area for each year were produced.

The processing of Sentinel-2 satellite imagery is a rigorous workflow designed to transform raw Top-Of-Atmosphere (TOA) data into scientifically viable Surface Reflectance (SR) products, which is a fundamental step for ensuring that temporal analyses are based on actual land surface changes rather than atmospheric artifacts. The primary objective of atmospheric correction is to eliminate the scattering and absorption effects caused by atmospheric gases and aerosols, typically achieved through the Sen2Cor processor. This process utilizes the libRadtran radiative transfer model to create Look-Up Tables (LUTs) that account for varying conditions of water vapor, ozone, and aerosol optical depth. By applying these corrections, the imagery is converted from Level-1C (TOA) to Level-2A (Bottom-of-Atmosphere) reflectance, ensuring the data represents the true physical properties of the Earth's surface, while also utilizing the 1.375 μm band to compensate for thin cirrus clouds that often elude standard detection methods. Accurate cloud and shadow detection serves as a critical prerequisite for any automated remote sensing pipeline, primarily managed through the Scene Classification Algorithm (SCA). This algorithm categorizes pixels based on multi-spectral thresholds, particularly focusing on high reflectance in the blue and short-wave infrared (SWIR) regions, while simultaneously projecting cloud shadows geometrically based on solar azimuth and elevation angles to generate high-quality Quality Indicators. While the standard SCL provides robust baseline classifications, researchers frequently augment this process with advanced machine learning approaches, such as the s2cloudless algorithm, which utilizes gradient-boosted trees to achieve superior precision in complex or heterogeneous landscapes.

To improve classification accuracy and eliminate erroneous change signals caused by phenological

changes, the LandTrendr algorithm, which performs pixel-based spectral trend analysis, was adapted and applied to the dataset created from Landsat satellite images. This algorithm examined the thirteen-year spectral trajectories of pixels, considering only areas showing statistically significant disturbance as real changes.

LandTrendr (Kennedy et al., 2010) is a remote sensing-based spectral-temporal segmentation algorithm designed to detect both abrupt and gradual land cover changes by analyzing Landsat satellite image time series through piecewise linear models. The operational mechanism begins with the generation of annual spectral index composites, such as NBR or NDVI, followed by a despiking process to filter noise and the identification of key vertices that represent significant breakpoints in the spectral trajectory. Mathematically, the algorithm fits an optimal piecewise continuous linear regression to the time series, defined as

$$\hat{y}_t = \beta_{0,j} + \beta_{1,j}t + \varepsilon_t \quad (2)$$

for each segment j , while maintaining a continuity constraint at each intersection point (t_v) such that $\beta_{0,j} + \beta_{1,j}t_v = \beta_{0,j+1} + \beta_{1,j+1}t_v$. By utilizing Ordinary Least Squares (OLS) to minimize the Sum of Squared Errors (SSE), LandTrendr iteratively simplifies complex models by removing weak vertices and evaluating statistical significance via an F-statistic. This reduction process adheres to the principle of Occam's Razor, ultimately selecting the simplest model that meets user-defined p-value thresholds to accurately represent the temporal evolution of the landscape.

Table 1. The key control parameters used for the Landtrendr algorithm.

Parameter	Value
Maximum Number of Segments	5
Vertex Count Overshoot Threshold	2
Spike Threshold	0.9
Recovery Threshold	0.25
P-Value Threshold	0.01
Best Model Proportion	1.25
Minimum Number of Observation	6

In order to guarantee complete transparency and the possibility of reproduction of the time-series analysis, the specific control parameters configured for the LandTrendr algorithm are detailed in Table 1. Furthermore, the temporal segmentation process is illustrated by Figure 7, which provides a schematic representation of a pixel's spectral trajectory. This demonstration shows how the algorithm filters out inter-annual noise (cloud masking and phenology differences) in order to identify permanent structural disturbances (breakpoints).

2.3.2. Change Detection

The study identified land cover transitions between 2017 and 2024 by applying the Raster Differencing method to time series data created from remote sensing images. Using the transition matrix created at this stage, the conversion from agricultural to urban areas, the loss of forest areas, and changes in water surfaces were calculated spatially and proportionally. In the Post-Classification Comparison phase, the Pixel-Based Coding method was applied to determine the direction and character of transitions between classes.

In this method, a new Change Raster was generated using the following formula, where the T2017 class values for the starting year are represented in the tens place and the T2024 class values for the ending year are represented in the ones place.

$$D_{pixel} = (S_{2017} * 10) + S_{2024} \quad (3)$$

Here, S_{2017} defines the land cover class value for 2017 (Class code: 3 (Agricultural Areas)), while S_{2024} defines the land cover class value for 2024 (Class code: 1 (Artificial Areas)). The matrix values obtained as a result of this process indicate that a pixel with code '31', which was Agriculture (3) in 2017, has been converted to Artificial Area (1) in 2024. Since the focus of the study is agricultural land loss, the analyses were specifically conducted on pixels with code '31'.

2.3.3. Spatial Characteristics and Edge Expansion Analysis

In classifying expansion types, the conceptual framework of the Landscape Expansion Index (LEI) developed by Liu et al. (2010), which is accepted as the fundamental reference in the literature, has been applied. A Distance to Nearest Hub analysis was performed using the QGIS program to determine the spatial distribution pattern and type of expansion of the identified urban transformation and land losses.

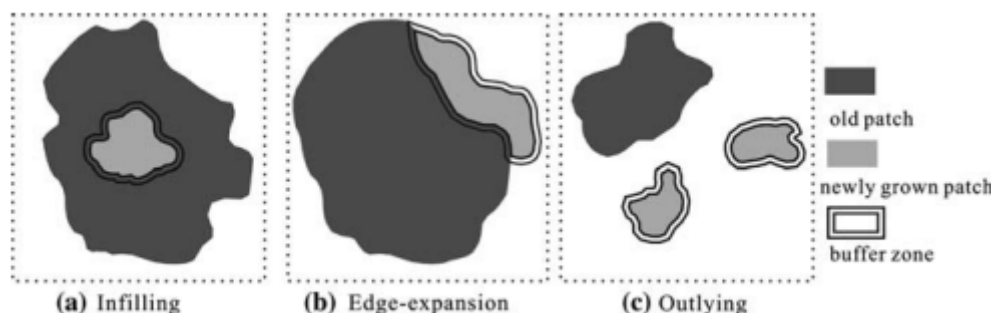


Figure 3. Types of land cover growth (Liu et al., 2010).

In this analysis, unlike traditional methods, the aim is to measure plan-discrepancy. Within this scope, the geometric centers (centroids) of polygons designated as Rural Residential Areas in the 1:25000 scale Master Development Plan data have been accepted as reference points (hubs). If the new de-

development area shares more than 50% of its boundary with the existing urban fabric, it is defined as infill development. If it shares between 0% and 50%, it is defined as edge expansion. If there is no shared boundary and the development is isolated, it is defined as leapfrog or outlying development.

In this study, the topological relationships in question were interpreted using a distance-based approach, and statistics (mean and median distance) were obtained by calculating the Euclidean distances of each pixel converted from agricultural to artificial land to these reference points. These statistics were used to determine whether the dominant growth characteristic in the region indicated a theoretically defined Jumping structure or Edge Expansion adjacent to existing plan boundaries (Figure 3). The threshold values used in the study were set as follows: infilling if the LEI index value is between $50 < LEI \leq 100$, Edge-Expansion if $0 < LEI \leq 50$, and Outlying (or leapfrog) if the LEI value is equal to 0.

2.3.4. Land Capability and Quality Analysis

Overlay analyses were performed to examine the physical nature of the change and the extent of agricultural loss. The productivity status of areas converted from agricultural use was determined by analyzing a change raster. This was done by overlaying it with digital data showing the Land Capability Classes belonging to the Ministry of Agriculture and Forestry. The pixels where loss or conversion occurred were then identified. As a result of this process, the proportion and area of land converted to Absolute Agricultural Land (Class I and II) and Marginal Agricultural Land have been calculated.

3. RESULTS

This section presents the results of hybrid analysis obtained using Sentinel-2 and Landsat satellite images under the headings of spatial change amount, comparison of methods, spatial characteristics of change, and relationship with land capability classes.

3.1. Basic Change Statistics and Method Comparison

The Random Forest classification method on the GEE platform with 100 decision trees was used to classify Sentinel-2 images from 2017 and 2024. The classification process was analyzed for accuracy, and the overall accuracy was determined to be 99.01%, 95.04%, and the kappa statistic was 0.98 and 0.89, respectively. The image difference detection method was used to identify changing classes within the time period, and areas that changed over the years were detected based on pixel changes. The difference image obtained as a result of the change detection process is shown in Figure 4.

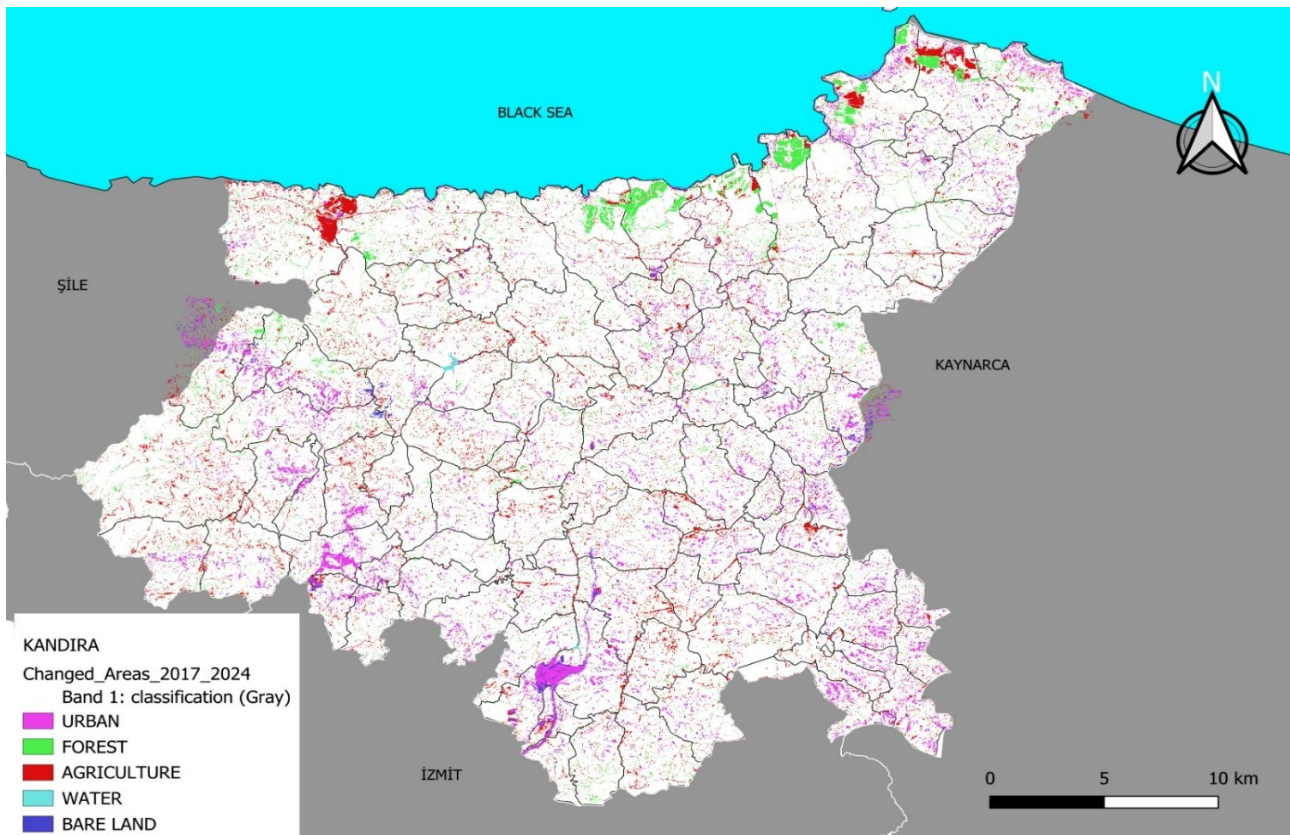


Figure 4. Changes in land cover/land use between 2017 and 2024.

Analyses covering the period 2017-2024 revealed that a total of 2,503 hectares (approximately 250,300 pixels) of agricultural land in the study area lost its character and was converted into artificial surfaces. This amount corresponds to approximately 2.6% of the agricultural land in the Kandira district. When examining the soil quality of the 2,503 hectares of land converted to non-agricultural use, it was observed that urban pressure was concentrated on low-yield agricultural land and medium-quality land. Distribution of change according to Land Capability classes the Marginal Agricultural Land class accounted for 50.7% of the total loss, making it the class that experienced the most intense conversion. This situation shows that development is shifting to the least resistant areas, taking into account the cost/efficiency balance. The Medium-Quality Land class accounts for 25.0% of the total loss. The uncertainty surrounding their protection status has left these lands vulnerable to development pressure. The share of Absolute Agricultural Land in the total conversion rate remained at 9.7% (Class I: 2.9%, Class II: 6.8%). This low rate indicates that the protective measures under Law No. 5403 have had a partial effect on absolute agricultural lands.

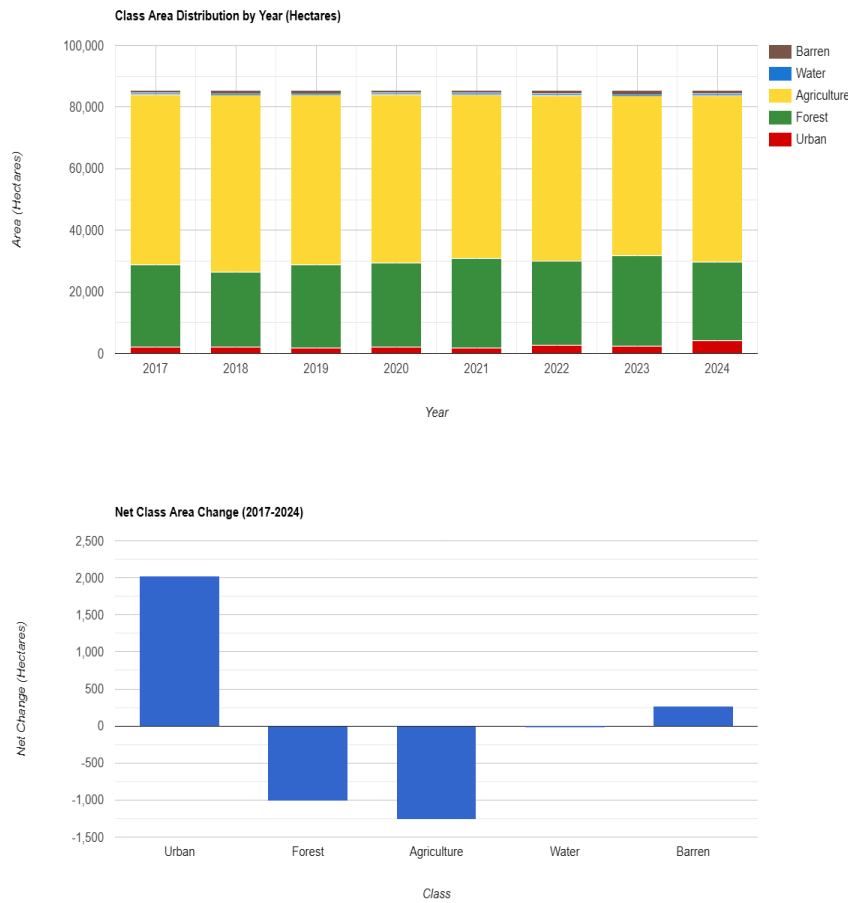


Figure 5. Changes in class area by year (top) and net changes in class area within years (bottom).

Figure 5 shows the significant changes between land cover classes in the study area during the 2017-2024 period. According to statistical calculations, the urban area, which was 2,065 hectares at the beginning of 2017, reached 4,179 hectares by 2024, indicating a net increase of 2,114 hectares (102.3%) in urban areas over a 7-year period. When examining the agricultural areas that form the main character of the region, it is seen that the agricultural land, which was 55,357 hectares in 2017, decreased to 53,897 hectares in 2024, resulting in a net loss of 1,459 hectares. Figure 4 also clearly shows that urbanization pressure is particularly evident in certain areas, especially in relation to the expansion of the Food Specialized Industrial Zone and the Kandıra-İzmit transportation route. Similarly, a decrease of approximately 970 hectares was observed in forest areas, with forest cover falling from 26,577 hectares to 25,607 hectares. However, interpreting changes in land cover solely based on net differences does not fully reflect the actual transformation parameters in the area. Analysis of the transition matrix created as a result of the classification reveals that the pressure of urbanization on agricultural areas is greater than the net change statistics indicate. The analysis results show that the 2,503-hectare area classified as agricultural land in 2017 will be converted into artificial areas by the end of 2024. According to these findings, the reason why the net agricultural loss reflected in the

statistics (1,459 ha) appears lower is understood to be a result of it being offset by partial transitions to agriculture from other classes (especially forest areas). Furthermore, the transition matrix created as a result of classification and change analysis demonstrates that the permanent conversion resulted in a gross loss of 2,503 hectares from agriculture to construction.

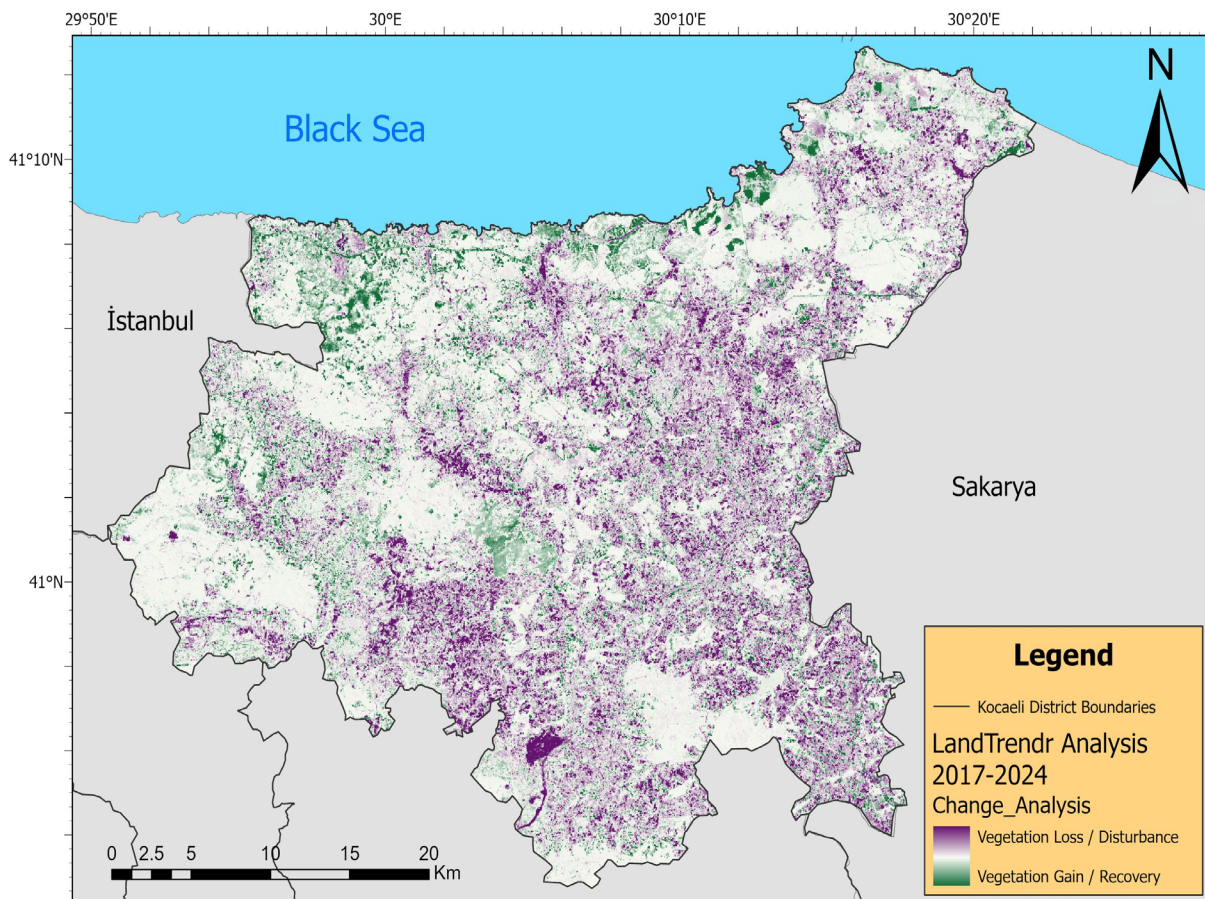


Figure 6. 2017 - 2024 Landtrendr analysis results for the study area.

The displayed values represent the spectral index difference (magnitude of change) and are unitless. Negative values (green areas) indicate vegetation growth or recovery, while positive values (purple areas) indicate a decrease in vegetation cover (disturbance or conversion to artificial surfaces).

The image obtained using the Landtrendr algorithm with Landsat 8 images from 2017 to 2024 is shown in Figure 6. The areas shown in purple in the figure represent the areas that have undergone change over time. Figure 7 shows the changes and graph related to the Food Organized Industrial Zone and highway construction carried out within the Kandira district in more detail. Figure 7 shows that a steady change in area has occurred over the years due to construction in the area shown in the black frame. It can be seen that the land cover areas in this region have changed over time and turned into urban areas. The descriptive outputs of LandTrendr are quantitatively supported by the

Random Forest post-classification transition matrix (Table 2). According to the cross-tabulation results between 2017 and 2024, exactly 2,503 hectares of agricultural land were directly converted into artificial surfaces, verifying the observed spectral disturbances.

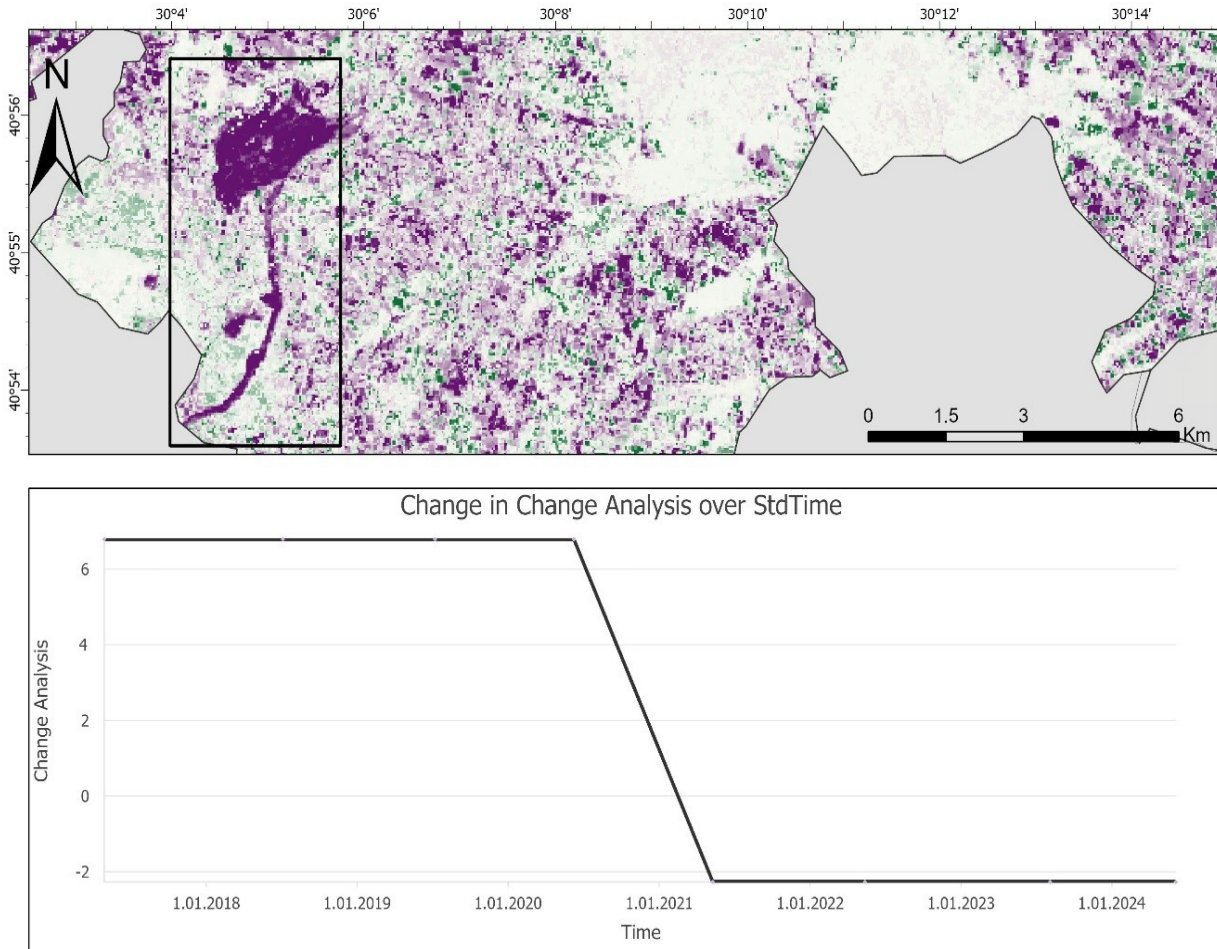


Figure 7. The change in a region within the study area over the years (transition from forest cover to urban).

Rather than establishing direct causality, a strong spatiotemporal correlation is observed. The breakpoints detected heavily after 2021 spatially and temporally coincide with the accelerated construction phases of major regional transportation infrastructures, such as the Izmit-Kandıra highway project and Kandıra Food Organized Industrial Zone (Güneş, 2022; KGM, 2022; Oktay, 2019).

When examining the annual change graphs (trajectory analysis) obtained with the LandTrendr algorithm, it was observed that vegetation loss (disturbance) did not follow a linear trajectory. The increase in breakpoints identified particularly in 2021 and beyond shows a temporal overlap with the construction processes of transportation projects (road widening and connecting roads) in the region. This finding reveals that land cover change is accelerated not only by housing demand but also by the triggering effect of large-scale infrastructure investments. When comparing the performance of

two different algorithms, Random Forest and LandTrendr, the spatial overlap level between Sentinel-2-based classification and Landsat-based time series analysis was calculated as a Jaccard Similarity Index of 10.41%. This coefficient reveals the spatial complexity of the transformation.

Table 2. Transition matrix of Random Forest classification.

2017 Class (From) \ 2024 Class (To)	Artificial Surfaces	Forest	Agriculture	Water Bodies	Barren Land	T o t a l 2017
Artificial Surfaces	1,261.93	18.80	547.58	5.40	119.76	1,953.46
Forest	38.26	23,290.97	3,087.99	3.59	37.85	26,458.70
Agriculture	2,503.02	2,104.01	50,505.73	28.26	576.89	55,717.90
Water Bodies	19.96	10.34	27.05	428.36	8.46	494.17
Barren Land	217.78	1.69	302.73	2.44	333.92	858.57
Total 2024	4,040.96	25,425.80	54,471.10	468.05	1,076.88	85,482.80

3.2. Spatial Distribution and Edge-Expansion

Secondly, the study analyzed the spatial distribution of changes in land cover. This analysis used LEI index values. When examining the spatial distribution pattern of areas transformed from agriculture to urban areas, it has been determined that the change does not exhibit random sprawl. The distances of conversion pixels to rural settlement centers (Hubs) were analyzed in the 1/25,000 scale Master Development Plan. The average distance was found to be 727 meters, while the median distance was 605 meters. The median value being lower than the average and the histogram clustering in the 0-1000 meter band statistically proves that new developments are not disconnected (leap-frog) from existing planned settlement areas, but rather spread by attaching to the peripheries of existing villages through the Edge-Expansion model.

The primary objective of the analysis is to determine whether the transformation occurred as leap-frog development independent of existing settlement areas, or as edge expansion adjacent to the existing fabric. First, the centroid of each pixel in the areas converted from agricultural land was created. Areas designated as rural residential areas in the 1/25000 scale Master Development Plan were also assumed to be hubs, and their centers of weight were determined pointwise and assigned as hub references. The Euclidean distance of each pixel converted from agriculture to urban was calculated to the nearest center (hub), and the median and mean of each distance total were calculated to find the central tendency, and the spread characteristic of the change was interpreted (Figure 8).

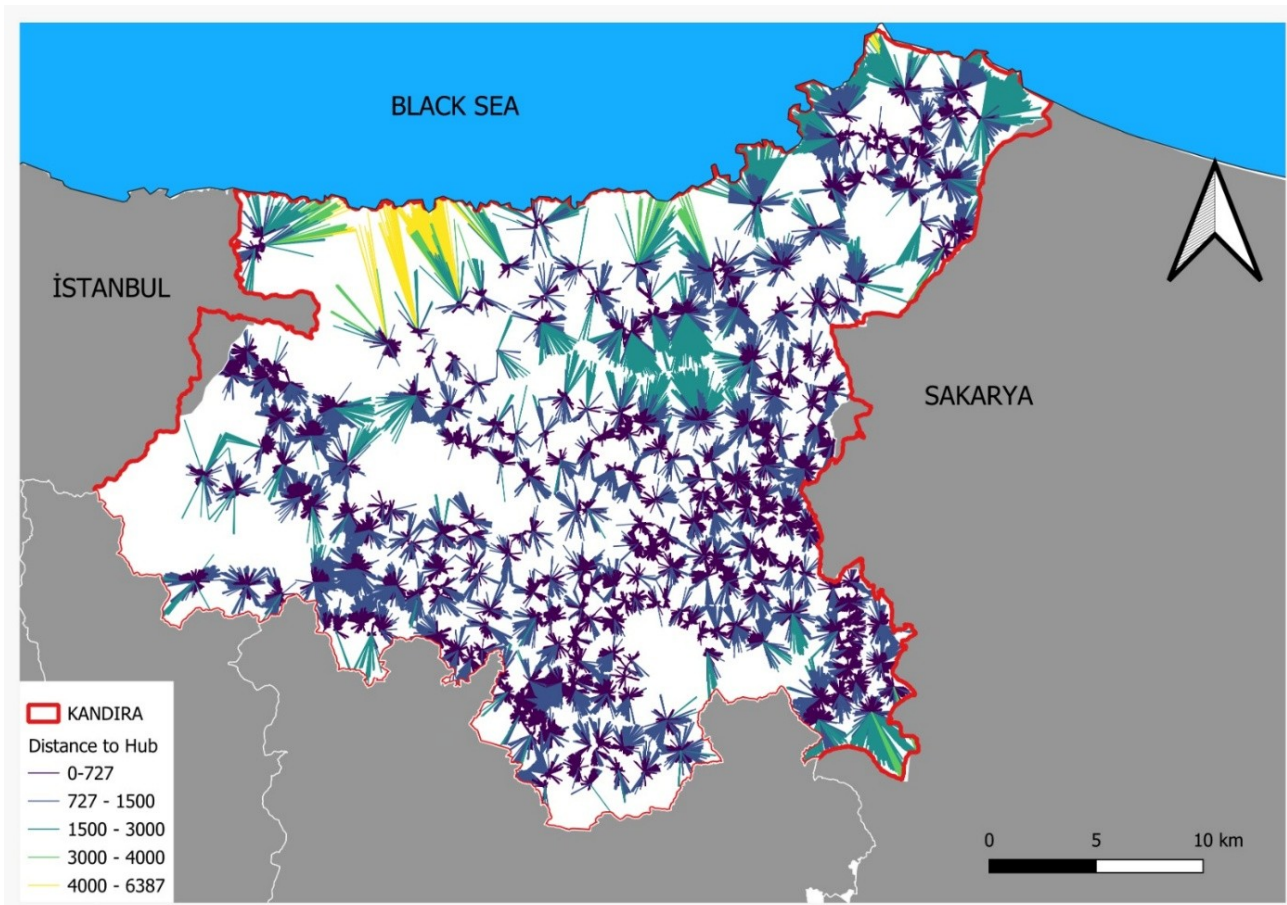


Figure 8. Land use/cover changes' spatial distribution.

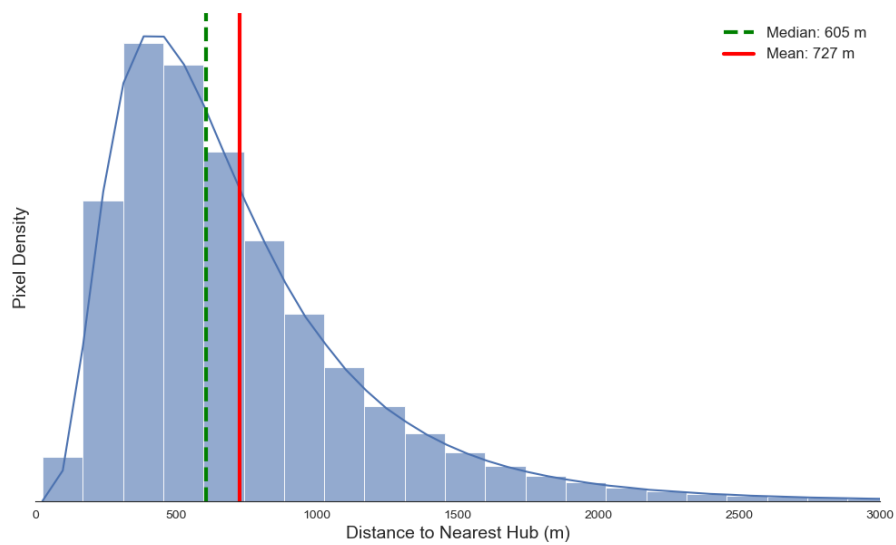


Figure 9. Distribution of distance from settlement centers to areas converted from agriculture to artificial land.

When examining Figure 8, it can be seen that the transition points indicated in dark blue (0-727 m) are particularly concentrated around residential areas. Examining the resulting histogram (Figure 9) revealed that the turning points accumulated around 605 meters and remained below the overall average value. The histogram in Figure 9 also supports this visual observation, showing that more than 60% of the conversion took place within a perimeter of 600-700 meters, which can be considered walking distance to the settlement center. It has been concluded that this loss of agricultural land has occurred in accessible agricultural areas immediately adjacent to planned rural settlements, and that urbanization tends to spread organically outward from existing centers.

The study examined the spatial distribution of areas converted from agricultural land to urban areas using the Landscape Expansion Index (LEI) as a reference (Figure 10). The topological computation revealed a highly fragmented transition pattern across the total 2,549.09 hectares of converted land. Edge-Expansion represents the largest proportion by area, accounting for 1,299.49 hectares (10,548 patches), indicating that a significant portion of the growth physically attaches to existing settlements and infrastructure. However, the Leapfrog expansion exhibits a striking pattern of rural fragmentation: although it covers slightly less area (1,098.05 hectares), it comprises the vast majority of individual patches (21,766 patches). This overwhelmingly high number of isolated leapfrog patches quantitatively proves that urbanization dynamics also manifest as thousands of disconnected, dispersed developments scattered across agricultural fields, indicating severe urban sprawl. Infilling represents the smallest proportion (151.55 hectares; 7,214 patches).

Integration of the Topological Landscape Expansion Index (LEI) with analyses of distance from the center demonstrates that significant agricultural loss in the designated area is attributable to the severe and uncontrolled nature of urban sprawl in the region. The findings indicate that Edge Expansion, encompassing 1,299 hectares, is the most predominant growth type in terms of area, suggesting that existing settlements are expanding in an outward direction. Nonetheless, in spite of its extensive coverage of 1,098 hectares, Leapfrog development encountered a substantial number of 21,766 isolated patches, thereby unveiling a pervasive degree of spatial fragmentation that has profoundly penetrated the underlying rural infrastructure. The evidence suggests that the distribution of these isolated artificial surfaces is not random but follows a systematic pattern, with a mean distance from official settlement centers of 727 meters (and a maximum of 6.3 kilometers). This pattern indicates that the phenomenon of leapfrog growth extends far beyond the planned boundaries of urban development. Consequently, the findings of the two analyses indicate with a high degree of clarity that the transformation of land in Kandira is not limited to the expansion of legal boundaries; on the contrary, this transformation directly threatens the sustainability of agriculture through unplanned urban sprawl that spreads across a multitude of disconnected fragments in the middle of agricultural land.

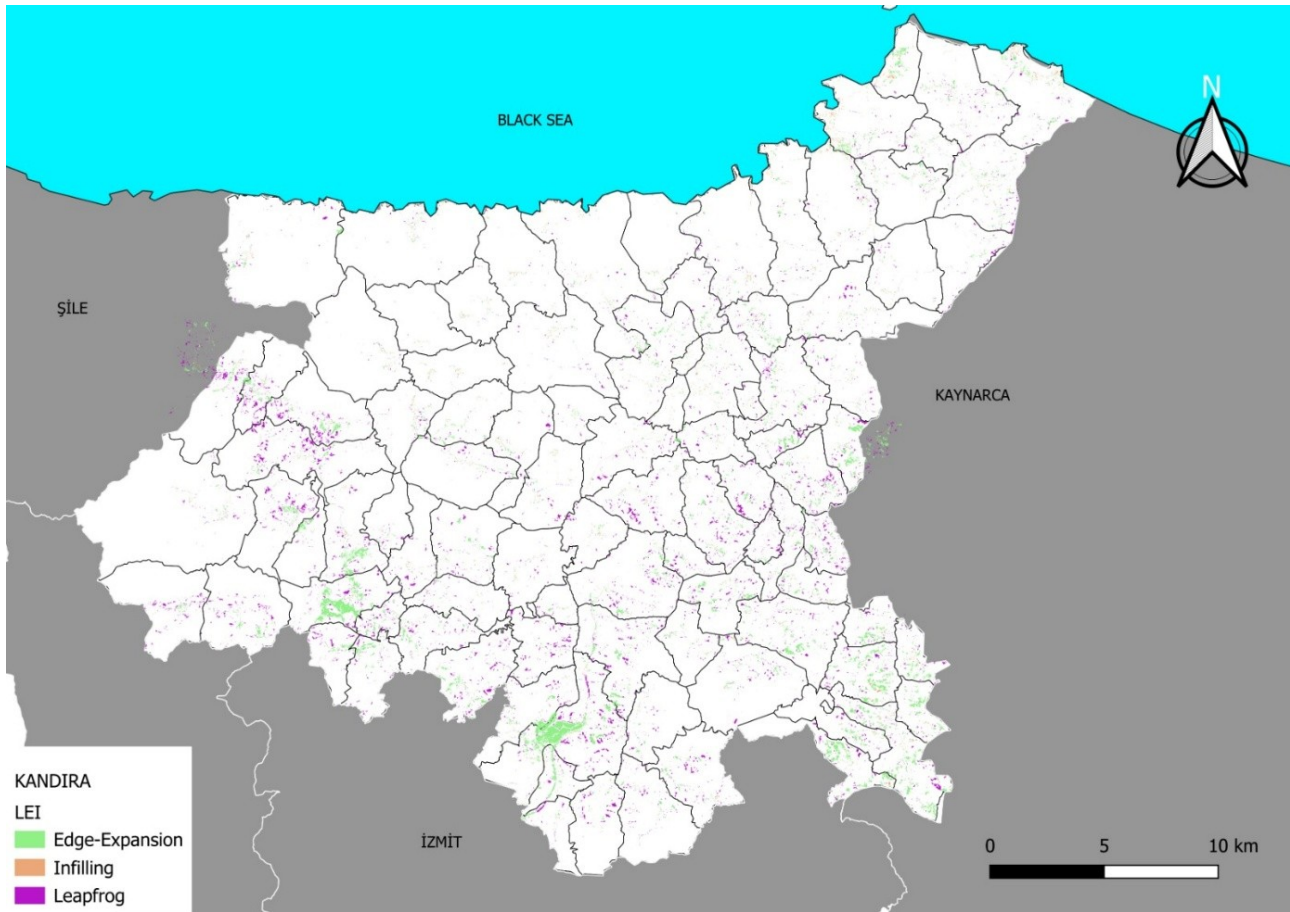


Figure 10. Landscape Expansion Index (LEI) analysis results.

4. DISCUSSION

The concept of resilience, which is increasingly being discussed in urban literature and urban policies, has begun to be expressed under several main headings. When the concept of resilience is evaluated specifically for the district of Kandıra in the province of Kocaeli, which is the study area, analyses have revealed that it is fragile in terms of ecological resilience. The fact that Kandıra district is relatively distant from major fault lines and more resilient to other disaster risks, as well as being adjacent to a megacity like Istanbul, has made the analyses conducted in this study indicative for the concrete calculation of the rapidly increasing urban pressure on rural areas following the pandemic. The Random Forest algorithm and Landtrendr analyses used in the study are understood to play a critical role in detecting changes in the spatial characteristics of the region and to be viable approaches for determining growth trends. Griffiths et al. (2013), used the LandTrendr algorithm with high accuracy in detecting abandoned deforestation as well as agricultural land. The findings obtained in this study also support the use of the algorithm in this direction. The spatial distribution of areas undergoing conversion from agriculture to artificial land in the study was found to be non-random when the spatial statistics were examined. The concentration of pixels undergoing transformation at an average distance of 727 meters from rural settlement centers identified in the 1/25,000 scale Mas-

ter Land Use Plan demonstrates that the urbanization dynamics in Kandıra exhibit the Edge-Expansion characteristic defined by Liu et al. (2010). This situation indicates a process in which agricultural land on the outskirts of existing villages is gradually incorporated into settlement areas, rather than the scattered leap-frog/outlying growth mentioned in the literature. Although this spatial dependency appears advantageous in terms of infrastructure costs, it demonstrates that planned settlement boundaries (village settlement areas) have effectively expanded at the expense of agricultural land and that the rural fabric is under pressure from urban sprawl. Furthermore, changes in land cover, as revealed by overlay analyses conducted using Land Capacity Classes, show partial alignment with the urban growth pattern described by Forman (1995) using the Path of Least Resistance approach. The fact that the conversion rate in Class I and II absolute agricultural lands, as stipulated by the Soil Conservation and Land Use Law No. 5403, remains at 9.7% suggests that deterrence measures for soil conservation in our country are functioning at a certain level. However, the high conversion rates of 50.7% in Class VI (marginal) lands and 25% in Class IV lands indicate that conservation pressure is shifting to weaker links. Given the current trend, this points to a gap in urban policy whereby, rather than rational and planned land selection taking place, agricultural land with potential (particularly Class IV) is left vulnerable or less resistant to urban pressure. The 2,503 hectares of land identified as having been converted from agriculture to artificial areas should not be viewed merely as a loss of vegetation. By increasing the cumulative heat load of these changing areas, it is also likely to have potential effects on the climate in the region. Indeed, studies conducted specifically in the province of Kocaeli (Akyürek, 2020) have clearly demonstrated a linear relationship between the increase in artificial surfaces and Land Surface Temperature (LST). This study also found that urban areas form distinct heat islands compared to rural environments. In this context, the areas identified in the study that have transitioned from agriculture to urban areas can be considered potential Hot Spots carrying the risk of thermal degradation, as indicated by Akyürek (2020). This transformation in an area that feeds Istanbul's climate corridor and water basin, such as Kandıra, is thought to accelerate regional ecological vulnerability in the long term, paving the way for ecological imbalance.

In this study, the high-resolution detections of the Sentinel-2 based Random Forest (RF) model were cross-validated using the Landsat-based Landtrendr time-series algorithm. The spatial agreement between the two algorithms was analyzed through a class-specific spatial masking technique. To achieve this, the continuous SWIR change magnitude values generated by the Landtrendr algorithm were thresholded and converted into a binary change mask. This binary mask was then multiplied pixel-by-pixel with the categorical RF map, which contained five distinct change classes (Urban, Forest, Agriculture, Water, Bare Land). Through this raster multiplication, only the pixels confirmed by Landtrendr in the time-series retained their original RF class values, allowing for the independent calculation of recall rates for each land cover category. The results demonstrated that the two methods exhibited a high rate of agreement (60%) in large-scale and permanent structural transformations, such as the Food Specialized Organized Industrial Zone. The spatial agreement between the the-

matic change map (RF) and the structural disturbance map (Landtrendr) was evaluated using the Jaccard Similarity Index, yielding a value of 0.104 (10.41%). While seemingly low for traditional single-sensor land cover comparisons, this value is highly expected and algorithmically justifiable in cross-methodological change detection frameworks (e.g., Cohen et al., 2018). This low spatial overlap stems from two fundamental disparities. First, the spatial mismatch between the 10-meter Sentinel-2 pixels and 30-meter Landsat pixels inherently reduces pixel-to-pixel intersection. Second, and more importantly, the two algorithms measure entirely different physical phenomena. Random Forest detects thematic land-cover conversion, whereas LandTrendr detects abrupt spectral structural disturbances. Therefore, rather than expecting a perfect spatial overlap, this study utilizes these two algorithms to capture different dimensions of the change: RF delineates the spatial typology and total area of urban expansion, while LandTrendr highlights the temporal trajectory and onset years of the vegetation disturbance.

5. CONCLUSION AND RECOMMENDATIONS

In our century, factors such as increasing migration due to globalization and global warming, the depletion of water resources, major fluctuations in agricultural production, and loss of biodiversity have made the sustainability of cities and the conservation of resources even more important. Undoubtedly, efforts to make cities sustainable and more resilient, as well as methods for measuring the effectiveness of these efforts, encompass many areas and methodologies. This study attempts to examine changes in rural land cover during the 2017-2024 period from an integrated perspective, combining cloud-based remote sensing technologies and spatial statistical methods. The spatial characteristics of the transformation were examined, determining the direction of the loss and the type of land cover affected, as well as identifying which agricultural lands experienced the greatest transformation in terms of agricultural productivity.

According to the findings of this study, it is important that conservation policies for sustainable land management be revised to include not only absolute agricultural lands but also Class IV lands, which have low resistance to urbanization and serve as buffer zones under urban pressure. In planning practice, rather than allowing the uncontrolled expansion of village settlement boundaries in response to the identified trend of Edge Expansion, it is necessary to implement Green Belt strategies that prioritize the preservation of the existing fabric and prevent sprawl. In addition, local governments or institutions responsible for spatial planning under the Ministry of Agriculture and Forestry can use LandTrendr, Sentinel and other high-resolution satellite images, or remote sensing systems with even higher resolution as an early warning system. This system can be used to detect and intervene in the destruction of agricultural areas before it reaches the stage of concretisation. This is important in terms of the effectiveness of rural planning, the protection of resources, and the prevention of vegetation loss.



REFERENCES

- Agaton, M., Setiawan, Y., & Effendi, H. (2016). Land use/land cover change detection in an urban watershed: a case study of upper Citarum Watershed, West Java Province, Indonesia. *Procedia Environmental Sciences*, 33, 654–660. <https://doi.org/10.1016/j.proenv.2016.03.120>
- Akyürek, Ö. (2020). Termal uzaktan algılama görüntüleri ile yüzey sıcaklıklarının belirlenmesi: Kocaeli örneği [Determination of surface temperatures with thermal remote sensing imagery: Kocaeli case]. *Doğal Afetler ve Çevre Dergisi*, 6(2), 377–390. <https://doi.org/10.21324/dacd.667594>
- Butt, A., Shabbir, R., Ahmad, S. S., & Aziz, N. (2015). Land use change mapping and analysis using Remote Sensing and GIS: A case study of Simly watershed, Islamabad, Pakistan. *The Egyptian Journal of Remote Sensing and Space Sciences*, 18(2), 251–259. <https://doi.org/10.1016/j.ejrs.2015.07.003>
- Chen, D., Wang, Y., Shen, Z., Liao, J., Chen, J., & Sun, S. (2021). Long time-series mapping and change detection of coastal zone land use based on Google Earth Engine and multi-source data fusion. *Remote Sensing*, 14(1), Article 1. <https://doi.org/10.3390/rs14010001>
- Cohen, W. B., Healey, S. P., Yang, Z., Stehman, S., Brewer, C., Brooks, E. B., Gorelick, N., Huang, C., Hughes, M. J., & Zhu, Z. (2017). How similar are forest disturbance maps derived from different Landsat time series algorithms? *Forests*, 8(4), Article 98. <https://doi.org/10.3390/f8040098>
- Drummond, M. A., & Loveland, T. R. (2010). Land-use pressure and a transition to forest-cover loss in the eastern United States. *BioScience*, 60(4), 286–298. <https://doi.org/10.1525/bio.2010.60.4.7>
- Forman, R. T. T. (1995). *Land mosaics: The ecology of landscapes and regions*. Cambridge University Press.
- Ghorbanian, A., Kakooei, M., Amani, M., Mahdavi, S., Mohammadzadeh, A., & Hasanlou, M. (2020). Improved land cover map of Iran using Sentinel imagery within Google Earth Engine and a novel automatic workflow for land cover classification using migrated training samples. *ISPRS Journal of Photogrammetry and Remote Sensing*, 167, 276–288. <https://doi.org/10.1016/j.isprsjprs.2020.07.013>
- Gorelick, N., Hancher, M., Dixon, M., Ilyushchenko, S., Thau, D., & Moore, R. (2017). Google Earth Engine: Planetary-scale geospatial analysis for everyone. *Remote Sensing of Environment*, 202, 18–27. <https://doi.org/10.1016/j.rse.2017.06.031>

- Griffiths, P., Müller, D., Kuemmerle, T., & Hostert, P. (2013). Agricultural land change in the Carpathian ecoregion after the breakdown of socialism and expansion of the European Union. *Environmental Research Letters*, 8(4), Article 045024. <https://doi.org/10.1088/1748-9326/8/4/045024>
- Gu, Y., Liu, T., Gao, G., Ren, G., Ma, Y., Chanussot, J., & Jia, X. (2021). Multimodal hyperspectral remote sensing: an overview and perspective. *Science China Information Sciences*, 64(12), Article 121301. <https://doi.org/10.1007/s11432-020-3084-1>
- Güneş, S. (2022, February 25). Kandıra İzmit yolunun 7 kilometrelik kısmı açıldı. *Kocaeli Gazetesi*. <https://www.kocaeligazetesi.com.tr/haber/9480672/kandira-izmit-yolunun-7-kilometrelik-kismi-acildi>
- Huang, H., Chen, Y., Clinton, N., Wang, J., Wang, X., Liu, C., Gong, P., Yang, J., Bai, Y., Zheng, Y., & Zhu, Z. (2017). Mapping major land cover dynamics in Beijing using all Landsat images in Google Earth Engine. *Remote Sensing of Environment*, 202, 166–176. <https://doi.org/10.1016/j.rse.2017.05.034>
- Kandıra District Governor's Office. (2025, December). Geographical location and landforms of Kandıra. T.C. Kandıra Kaymakamlığı. <https://www.kandira.gov.tr/cografi-konumu-ve-yeryz-sekilleri>
- Karayolları Genel Müdürlüğü. (2022, June). İzmit-Kandıra-Kaynarca Yolu, Çubuklubala-Çubuklu Osmaniye Varyantı ile Cezaevi Varyantı. T.C. Ulaştırma ve Altyapı Bakanlığı. <https://www.kgm.gov.tr/Sayfalar/KGM/SiteTr/Projeler/ProjelerDetay.aspx?q=87>
- Kennedy, R. E., Yang, Z., & Cohen, W. B. (2010). Detecting trends in forest disturbance and recovery using yearly Landsat time series: 1. LandTrendr—Temporal segmentation algorithms. *Remote Sensing of Environment*, 114(12), 2897–2910. <https://doi.org/10.1016/j.rse.2010.07.008>
- Kennedy, R. E., Yang, Z., Gorelick, N., Braaten, J., Cavalcante, L., & Cohen, W. B. (2018). Implementation of the LandTrendr algorithm on Google Earth Engine. *Remote Sensing*, 10(5), Article 691. <https://doi.org/10.3390/rs10050691>
- Kongar, E. (2002). 21. Yüzyılda Türkiye: 2000'li yıllarda Türkiye'nin toplumsal yapısı. *Remzi Kitabevi*.
- Li, X., & Yeh, A. G. O. (2004). Analyzing spatial restructuring of land use patterns in a fast growing region using remote sensing and GIS. *Landscape and Urban Planning*, 69(4), 335–354. <https://doi.org/10.1016/j.landurbplan.2003.10.033>
- Li, Y., Liu, C., Zhao, W., & Huang, Y. (2020). Multi-spectral remote sensing images feature coverage classification based on improved convolutional neural network. *Mathematical Biosciences and Engineering*, 17(5), 4443–4456. <https://doi.org/10.3390/mbe.2020245>



- Liu, X., Li, X., Chen, Y., Tan, Z., Li, S., & Ai, B. (2010). A new landscape index for quantifying urban expansion using multi-temporal remotely sensed data. *Landscape Ecology*, 25(5), 671–682. <https://doi.org/10.1007/s10980-010-9454-5>
- Nguyen, L. B. (2020). Land cover change detection in northwestern Vietnam using Landsat images and Google Earth Engine. *Journal of Water and Land Development*, 46, 162–169. <https://doi.org/10.24425/jwld.2020.134209>
- Okoduwa, A. K., & Amaechi, C. F. (2024). Exploring Google Earth Engine, Machine Learning, and GIS for Land Use and Land Cover Change Detection in the Federal Capital Territory, Abuja, between 2014 and 2023. *Applied Environmental Research*, 46(2), Article 029. <https://doi.org/10.35762/AER.2024029>
- Oktaç, Ş. (2019, September 22). Kandıra Gıda İhtisas OSB binlerce kişiye ekmek kapısı olacak. *Anadolu Ajansı*. <https://www.aa.com.tr/tr/ekonomi/kandira-gida-ih-tisas-osb-binlerce-kisiye-ekmek-kapisi-olacak/1590579>
- Pande, B. C. (2022). Land use/land cover and change detection mapping in Rahuri watershed area (MS), India using the Google Earth Engine and machine learning approach. *Geocarto International*, 37(26), 13860–13880. <https://doi.org/10.1080/10106049.2022.2086622>
- Rogan, J., & Chen, D. M. (2004). Remote sensing technology for mapping and monitoring land-cover and land-use change. *Progress in Planning*, 61(4), 301–325. [https://doi.org/10.1016/S0305-9006\(03\)00066-7](https://doi.org/10.1016/S0305-9006(03)00066-7)
- Szeliski, R. (2022). *Computer vision: Algorithms and applications* (2nd ed.). Springer. <https://doi.org/10.1007/978-3-030-34372-9>
- Teja, J., Vaddi, R., Lakshmika, K., & Nirupama, P. (2024, April 24–26). Land use and land cover change detection using Google Earth Engine [Paper presentation]. 7th International Conference on Inventive Computation Technologies (ICICT 2024), Lalitpur, Nepal.
- Tırmanoğlu, B., İsmailoğlu, İ., Kokal, A. T., & Musaoğlu, N. (2023). Yeni nesil multispektral ve hiperspektral uydu görüntülerinin arazi örtüsü/arazi kullanımı sınıflandırma performanslarının karşılaştırılması: Sentinel-2 ve PRISMA Uydusu [Comparison of land cover/land use classification performances of next-generation multispectral and hyperspectral satellite imagery: Sentinel-2 and PRISMA Satellite]. *Geomatik*, 8(1), 79–90. <https://doi.org/10.29128/geomatik.1126685>
- Tobler, W. R. (1970). A computer movie simulating urban growth in the Detroit region. *Economic Geography*, 46, 234–240. <https://doi.org/10.2307/143141>